

# Eurasia spreading basin to Laptev Shelf transition: structural pattern and heat flow

S. S. Drachev,<sup>1</sup> N. Kaul<sup>2</sup> and V. N. Beliaev<sup>3</sup>

<sup>1</sup>*Institute of Lithosphere of Internal and Marginal Seas, Russian Academy of Sciences, 120, Moika Embankment, St Petersburg, 190121, Russian Federation. E-mail: sdrachev@mail.ru*

<sup>2</sup>*University of Bremen, Geosciences, Klagenfurter St, 28334 Bremen, Germany. E-mail: nkaul@geophys2.uni-bremen.de*

<sup>3</sup>*Marine Arctic Geological Expedition, 26 Sofia Perovskaya St, Murmansk, 183012, Russian Federation. E-mail: mage@com.mels.ru*

Accepted 2002 September 16. Received 2002 September 6; in original form 2001 September 7

## SUMMARY

New geophysical data have become available from shipborne and satellite measurements allowing a re-evaluation of the largely unknown junction of the Arctic spreading centre and the northeastern Siberian continental margin where the transpolar mid-ocean Gakkel Ridge abuts against the continental slope of the Laptev Sea. Based on multichannel seismic reflection and gravity data, this sediment-covered spreading axis can be traced to the continental rise where it is cut-off by a transcurrent fault. Further continuation of the extensional axis into the continental slope can be attributed to two asymmetric grabens, which terminate against the prominent Khatanga–Lomonosov Fracture. Remnants of hydrothermal fauna and high heat-flow values of approximately  $100 \text{ mW m}^{-2}$  documented around these grabens in the up-slope area are typical for an oceanic spreading axis. Thus we consider these grabens to be morphotectonic termination of the global Atlantic–Arctic spreading system with plate motions shifting to the Khatanga–Lomonosov Fracture. The high heat flow and the distribution of earthquake epicentres allow us to assume that the present-day divergent plate tectonic boundary passes from the Gakkel Ridge to the eastern part of Laptev Sea with an offset of initial rifting along the Bel'kov–Svyatoi Nos Rift to the projected prolongation of the buried spreading axis by 140–150 km.

**Key words:** Eurasia Basin, heat flow, Laptev Sea, ocean–continent transition, rifts, spreading.

## INTRODUCTION

Areas of transition from rifting to spreading are of increasing interest for Earth's scientists (see, for example, the MARGINS initiative Science Plan at <http://www.ideo.columbia.edu/margins/SciPlan.html>). These sites are regarded as crucial to the study of active processes of breakup of supercontinents and the origin of Atlantic-type passive continental margins, including large-scale and meso-scale lithospheric deformations, mantle processes and their environmental impact. At present, active seafloor spreading is converting into a continental rifting in the Gulf of Suez and the Gulf of Tadjoura in the Red Sea region, the Gulf of California in North America, Woodlark Basin in Papua New Guinea and in the Siberian Laptev Sea. The latter is situated between the Taimyr Peninsula and the New Siberian Islands at the eastern end of the Eurasia basin (Fig. 1), where the slowest spreading ridge on the Earth (the Gakkel Ridge) abuts against the Laptev Sea continental margin (LSCM).

The concept of the Gakkel Ridge extension into the Laptev Shelf was initially proposed by Dementitskaya & Karasik (1969) and Grachev *et al.* (1970) after the spreading nature of the Eurasia Basin was recognized. The LSCM was considered to be a transitional zone of crustal extension between the Gakkel Ridge and the intraconti-

ental Moma Rift in internal Northeastern Asia (Zonenshain *et al.* 1978; Grachev 1982). Nevertheless, this area has for a long time remained an enigmatic site of rift to drift transition since the spreading ridge/continental margin intersection occurs entirely under a remote ice-covered northern sea. Before the mid-1980s the outline of the predicted rift system beneath the shelf could only be roughly delineated by interpretation of the bathymetry, seismicity, potential field surveys and limited seismic refraction data (Patyk-Kara & Grishin 1972; Grachev 1982; Vinogradov 1984; Fujita *et al.* 1990a). Much less was known of where and how the Gakkel Ridge intersects the continental margin. Moreover, although the Moma Rift and surrounding Cherskii Arch are characterized by high heat flow and the presence of thermal springs (Parfenov *et al.* 1988), no heat-flow measurements had been conducted at the LSCM.

A breakthrough in understanding of LSCM geology was achieved by marine multichannel seismic reflection (MCS) surveys. On a small scale they were started by the Russian geophysical company MAGE (Marine Arctic Geological Expedition, Murmansk) in 1984 and were continued by MAGE in 1986, 1987 and 1990, LARGE (Laboratory of Regional Geodynamics, Moscow) and SMNG (Sevmorneftegeofisika, Murmansk) in 1989, BGR (Federal Institute for Geosciences and Natural Resources, Hannover, Germany)

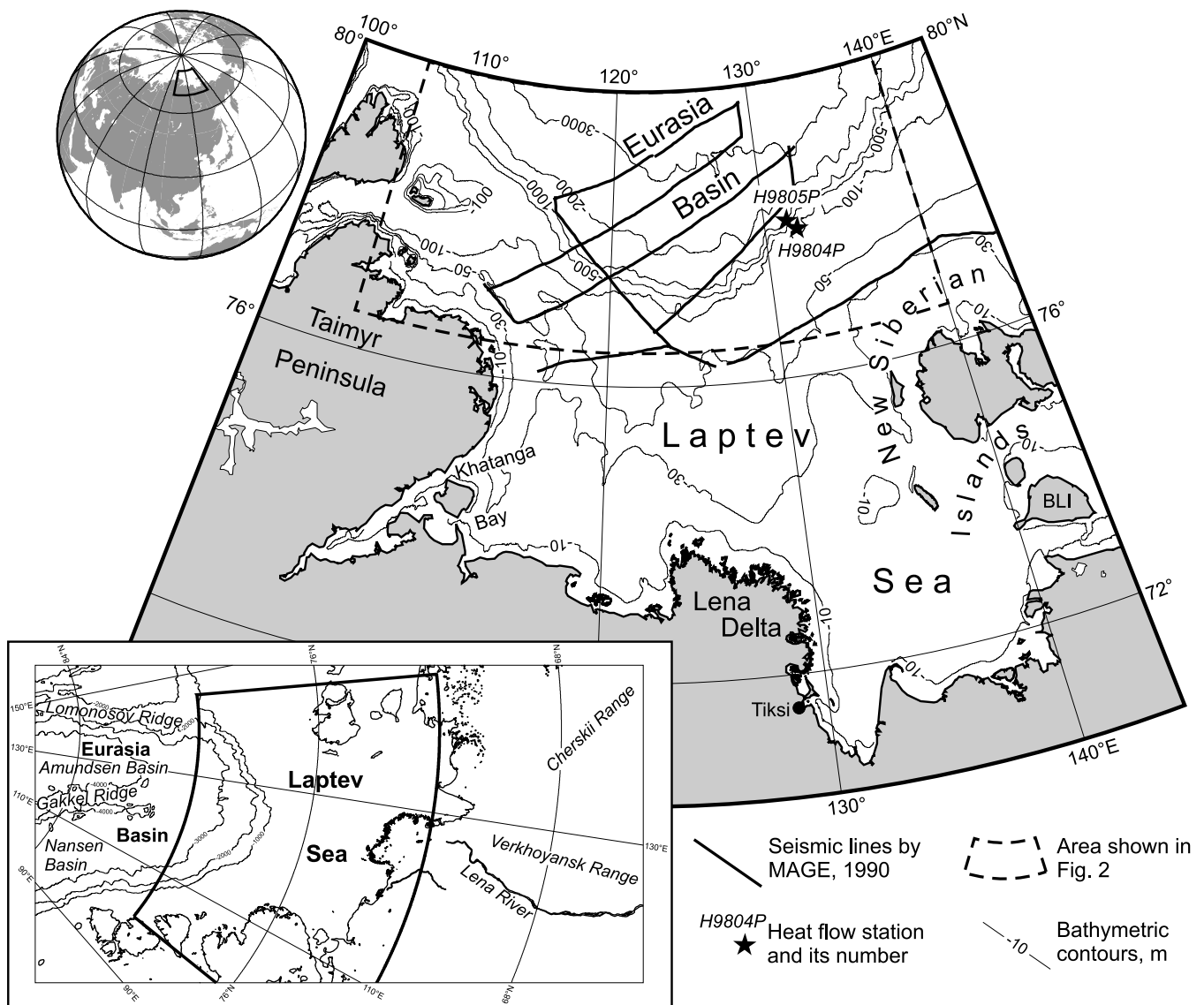


**Figure 1.** Index map of the Laptev Sea region showing location of sites of heat flow measurements conducted onboard *FS Polarstern* and multichannel seismic reflection profiles by MAGE's 1990 survey (polar stereographic projection, IBCAO bathymetry after Jakobsson *et al.* 2000). The globe and a small-scaled insertion show the location of the studied area. BLI—Bol'shoi Lyakhov Island.

in cooperation with SMNG in 1993, 1994 and 1997, and within the framework of the Russian–German cooperative programme 'Laptev Sea System 2000' in 1998. These studies allowed a better delineation of the predicted Laptev Rift system (Ivanova *et al.* 1990; Roeser *et al.* 1995; Drachev 1998, 2000; Drachev *et al.* 1998; Franke *et al.* 1998, 2001).

The drastic improvement in our understanding of the Gakkel Ridge/LSCM intersection is mainly due to the MAGE 1990 survey, the MCS profiles of which crossed the eastern Eurasia Basin between 77°–80°N and 115°–133°E north of the Laptev Shelf (Sekretov 2002, see fig. 1 for the survey location). In subsequent years a new insight into the tectonic fabric of this region was derived from an unprecedented gravity field obtained by means of satellite ERS-1 and ERS-2 altimetry (Laxon & McAdoo 1994, 1998). Finally, first heat-flow measurements were performed from the German *FS Polarstern* in 1998 as part of the recently concluded programme 'Laptev Sea System 2000'. This paper presents the results of these studies, which help to define the main structural characteris-

tics and heat-flow values of the Gakkel Ridge at its junction with the LSCM.

### TECTONIC SETTING AND STRUCTURE OF THE EURASIA BASIN IN THE VICINITY OF THE LAPTEV SEA CONTINENTAL MARGIN

The Eurasia Basin is an oceanic basin created by seafloor spreading over the previous 53–56 Myr (Karasik 1974; Vogt *et al.* 1979; Kristoffersen 1990). Its spreading axis, the Gakkel Ridge, separates the North American and Eurasian lithospheric plates in the Arctic and represents an ultraslow spreading ridge with recent spreading taking place close to a pole of plate rotation at approximately the Lena Delta (Cook *et al.* 1986; Franke *et al.* 2000). This position of the pole of rotation is derived entirely from seismological studies and brings it back on to the continent, in opposition to the northern position at the shelf break found by Argus & Heflin (1995). The

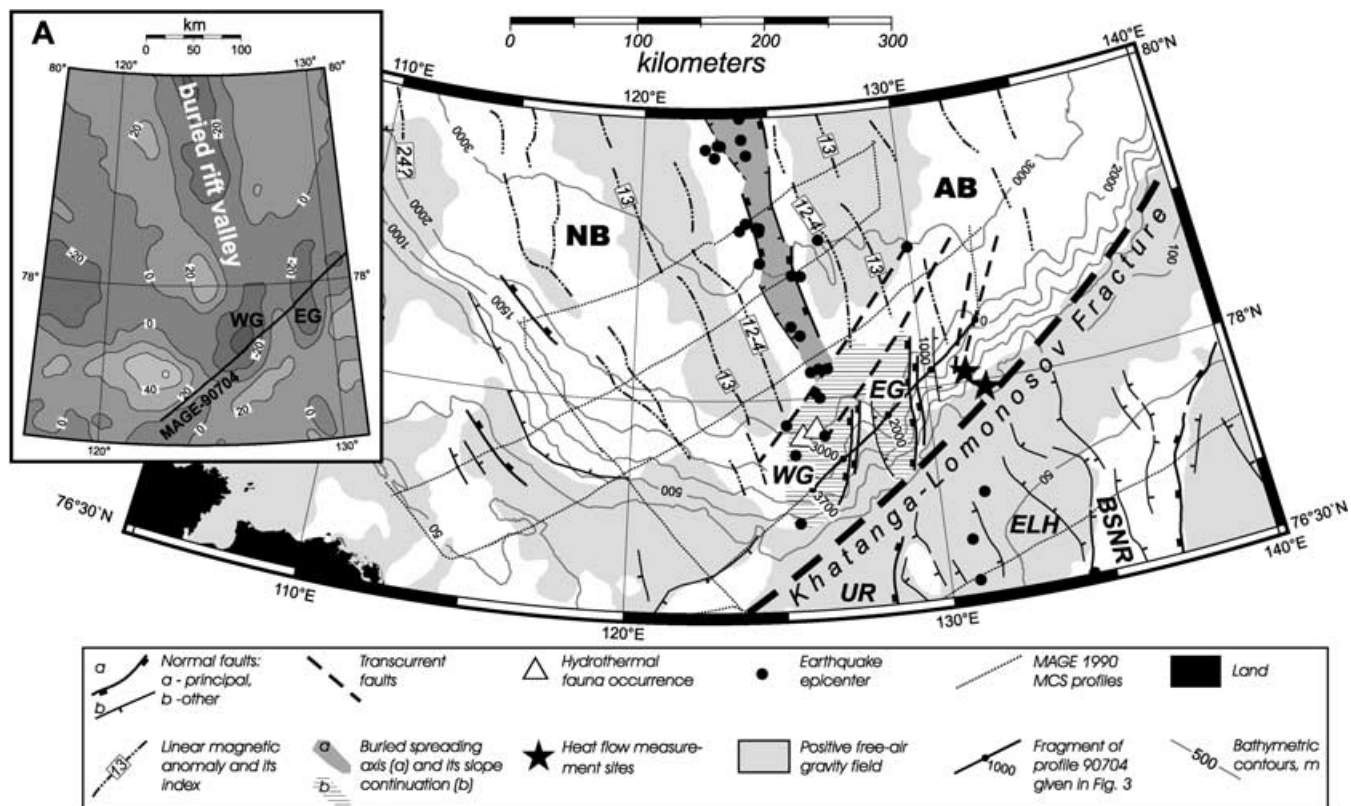


**Figure 2.** Structural pattern of the Eurasia Basin–Laptev Shelf transition area (polar stereographic projection, IBCAO bathymetry). NB—Nansen Basin, AB—Amundsen Basin, WG—Western Graben, EG—Eastern Graben, UR—Ust’ Lena Rift, ELH—East Laptev Horst, BSNR—Bel’kov–Svyatoi Nos Rift. Axis of linear magnetic anomalies are given after Karasik & Sochevanova (1990). The light grey indicates a positive free-air gravity field of 0 to 60 mGal, and the white background corresponds to negative field of 0 to –50 mGal as corresponds to a chart (A) at the right upper corner (gravity data provided by D. McAdoo 2000). The seismicity data were extracted from National Earthquake Information Center database, US Geological Survey (<http://eqint.cr.usgs.gov>).

finite opening rate in the Eurasia Basin decreases from approximately  $16.5 \text{ mm yr}^{-1}$  near Greenland to  $6 \text{ mm yr}^{-1}$  at its Laptev termination (DeMets *et al.* 1990). The eastward-directed degeneration of the spreading along the Gakkel Ridge is also well consistent with aeromagnetic data (Karasik 1974; Vogt *et al.* 1979; Karasik *et al.* 1983).

The available net of aeromagnetic track lines (Verhoef *et al.* 1996; Glebovsky *et al.* 2000) covers most of the Eurasia Basin. A well-detectable set of linear magnetic anomalies ranged from A24 to A0 in the central part of the basin loses its distinctiveness towards the Laptev Sea where the data coverage and resolution decrease. The magnetic field in the vicinity of the LSCM reveals a weak and poorly differentiated linearity, which is quasi-symmetric about an axial negative anomaly. This is considered to be mainly a consequence of very slow spreading, resulting in merging (overlapping) adjacent anomalies (Karasik 1974). According to Karasik & Sochevanova (1990), only anomaly 13 (33 Ma). The age of magnetic anomalies is given after Cande & Kent (1995), which is a prominent anomaly in the North Atlantic and Arctic regions, can be identified in this area with confidence.

The near-Laptev part of the Eurasia Basin south of  $80^\circ\text{N}$  has received a large amount of terrestrially derived sediments, supplied by several large Siberian rivers, of which the Lena River is the largest. According to the MAGE MCS profiles (Sekretov 2002), a thick sedimentary cover spreads down to 3500 m isobath and further into the ocean basin, burying the basement topography of the Eurasia Basin. The Gakkel Ridge is vanishing almost completely under this Siberia-derived sedimentary pile at *ca.*  $80^\circ40'\text{N}$ ,

$122^\circ\text{E}$ , representing a rare case of an active sediment-covered ridge.

The buried Gakkel Ridge is manifested on seismic profiles as a high-standing block of acoustic basement complicated by a median rift valley (Sekretov 2002). The thickness of the overlying sediments varies from 0.4 km over the flanks of the buried ridge to 6–7 km above the rift valley and in the surrounding oceanic basins. The buried rift valley is clearly displayed in the free-air gravity field as a distinct linear low (–20 to –50 mGal) surrounded by linear highs from 10 to 50 mGal (Laxon & McAdoo 1998; Drachev *et al.* 1999). The latter are obviously related to the flanks of the buried ridge (Fig. 2a).

Based on MCS and gravity data, the buried spreading axis (BSA) is traced to the continental rise up to  $78^\circ22.6'\text{N}$   $126^\circ05.3'\text{E}$  where it terminates against an oblique transcurrent fault. At the apparent upslope continuation of the BSA there are two isolated gravity minima. They are crossed by the seismic line MAGE-90704 and, as follows from the MCS data, are correlated to asymmetric grabens (Fig. 3). Some of the normal faults bordering the grabens reach up to the sea bottom, affecting its morphology and providing evidence of recent tectonic activity, which is supported by the seismicity.

Both the BSA and its upslope continuation are seismically active (Fig. 2). For most of the events the extensional focal mechanisms with a fault plane oriented along the rift valley are determined (Savostin & Karasik 1981; Parfenov *et al.* 1988; Fujita *et al.* 1990b; Avetisov 1999). The earthquake epicentres are clustered along the normal faults that border the sediment-covered rift valley. A separate cluster is located at the termination of the BSA on its intersection

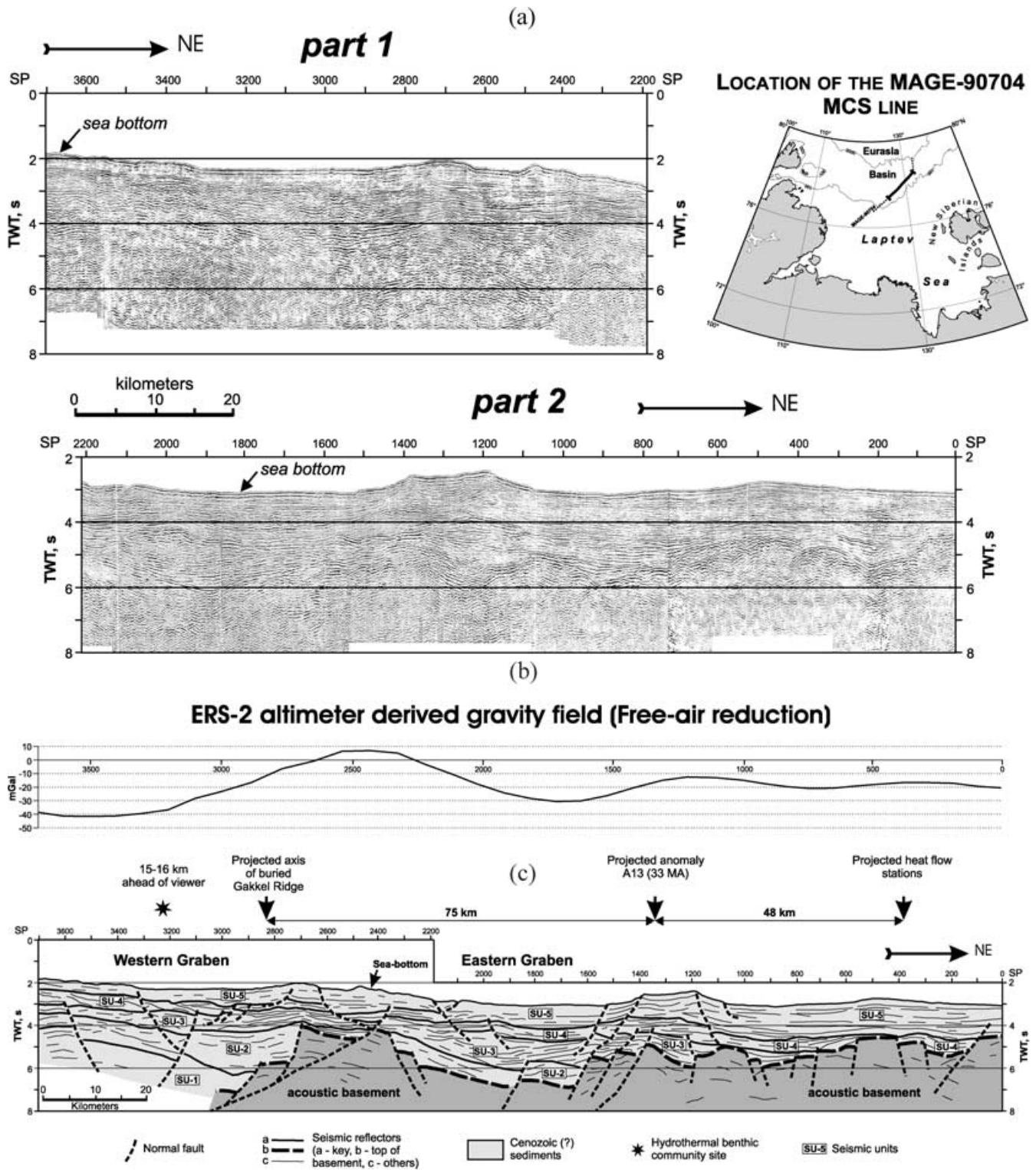


Figure 3. A 186 km long fragment of seismic reflection line MAGE-90704 (A) followed by free-air gravity chart (B) and a line-drawing (C) showing subbottom extensional structure and sediment distribution at the upslope continuation of the Gakkel Ridge buried spreading axis. Position of the seismic line is given in Figs 2 and 3(A). Gravity field is provided by D. McAdoo (2000).

with the transcurrent fault. South of this site the strip of epicentres turns to the Western Graben, and then passes over on to the shelf where seismicity is widely distributed following the main rift zones as Ust' Lena and Bel'kov-Svyatoi Nos rifts (Drachev 1998; Avetisov 1999; Franke *et al.* 2000).

The Khatanga-Lomonosov Fracture striking from the Khatanga River Inlet to the shelf edge of the Amundsen Basin is a major SW-NE-trending transcurrent fault, which probably represents a sheared boundary between the spreading-dominated Eurasia Basin and the continental rift system of the Laptev Shelf (Drachev *et al.*

**Table 1.** Results of heat-flow measurements on the Laptev Sea continental slope.

Site no	Date	Long., E	Latitude, N	Water depth (m)	T. grad (mK m <sup>-1</sup> )	Therm. cond. (W mK <sup>-1</sup> )	Heat flow, (mW m <sup>-2</sup> )	Heat flow corr. (mW m <sup>-2</sup> )
H9804P01	7.8.98	132°03.61'	77°56.00'	514.6	86	0.9–1.1	87	102
H9804P02	7.8.98	132°03.26'	77°56.02'	529.4	92	0.9–1.1	100	117
H9804P03	7.8.98	132°03.09'	77°56.07'	537.1	92	0.9–1.1	92	108
H9805P01	8.8.98	131°25.67'	78°03.83'	1568.0	92.6	0.9–1.1	73	85
H9805P02	8.8.98	131°26.62'	78°03.90'	1554.0	92.8	0.9–1.1	84	98
H9805P03	8.8.98	131°27.35'	78°03.94'	1541.0	94	0.9–1.1	86	101

1998). This fracture cuts off the Western and Eastern grabens in the upper continental slope. Further on the shelf a zone of recent plate divergence can be attributed to a pronounced branch of the epicentres found east of the East Laptev Horst along the northern part of Bel'kov–Svyatoi Nos Rift. Thus there is a left-hand offset of approximately 140–150 km along the Khatanga–Lomonosov Fracture between the BSA and the recently active easternmost rift of the Laptev Rift system.

In the area of the Western Graben (Fig. 2) fossil bivalve shells of the family *Vesicomidae* were found in 1993 and 1995 during *FS Polarstern* cruise ARK-IX/a (Fütterer 1994; Petryashov *et al.* 1994; Sirenko *et al.* 1995). The species of the family *Vesicomidae* are among typical representatives of benthic communities known from hydrothermal sites of mid-oceanic ridges. According to Petryashov *et al.* (1994) the retrieved species are similar to *Archivesica inflata* from the Gulf of California. C<sup>14</sup> dating performed by the Leibniz Laboratory (Kiel, Germany) revealed an age of an *Archivesica sp.* shell of approximately 15.7 kyr (B. Kim, *Pers. comm.*, 2000).

Thus these unique faunal findings suggest the recent occurrence of hydrothermal activity in the lower continental slope. This, in turn, provides good evidence for a continuation of the Gakkel Ridge divergent axis into the continental slope of the LSCM. The high heat-flow values close to the Eastern Graben (Fig. 2) support this suggestion.

#### HEAT-FLOW MEASUREMENTS: INSTRUMENTATION AND DATA DESCRIPTION

During *FS Polarstern* cruise ARK XIV 1/b, a Lister-type heat-flow probe (Hyndman *et al.* 1979) was used to measure the temperature gradients down to 3.5 m below the sea bottom. This instrument of violin bow design is capable of performing *in situ* thermal conductivity measurements using a pulsed heat source method. The active

length of the sensor string is 3 m with 11 thermistors spaced every 0.3 m.

Measurements at a station have been made using a set of three individual penetrations to gain reliable results, even in the case of lateral heat-flow variability or measurement deficiencies. Processing of the raw data is done according to an inversion method, developed by Hartmann & Villingger (2002). The thermal conductivity is calculated from heat pulse decay. Nine stations have been investigated in total, seven on the shallow shelf and two, which are relevant for this survey, on the continental slope. The results of six penetrations on these two stations (H9804 and H9805) are presented in Table 1. These two stations on the continental slope are of particular importance, because permanent pack ice prevents easy access to more northerly locations and a shallow shelf to the south prevents access to an undisturbed geothermal gradient of those heat-flow stations there.

Station H9804 is located on the continental slope at 515–540 m water depth. This is below the lowermost sea level stand that has ever occurred in this region (–120 m after Bauch *et al.* 1999). From conductivity, temperature, depth (CTD) measurements it is known that warm Atlantic intermediate water masses flow into the Arctic Ocean and influence the depth section between 100 and 800 m (Rudels *et al.* 1994). So station H9804 is free of terrestrial influx but possibly suffers from oceanographic effects, which are variable in time and depth range. Figs 4(a)–(c) depicts the results of three penetrations (H9804P01–H9804P03), which are approximately 100 m apart. The gradients are not linear along the complete penetration depth, indicating a distortion caused by near-bottom water within the recent past. The lowermost three temperature readings are considered to be reasonably linear to represent the geothermal heat flux. The thermal conductivity is assumed to be 1.1 W mK<sup>-1</sup>.

The second station H9805 is further down the continental slope at 1541–1568 m water depth. According to a CTD cast, this water depth is well below the influx of Atlantic mid-water inflow. Figs 4(d)–(f)

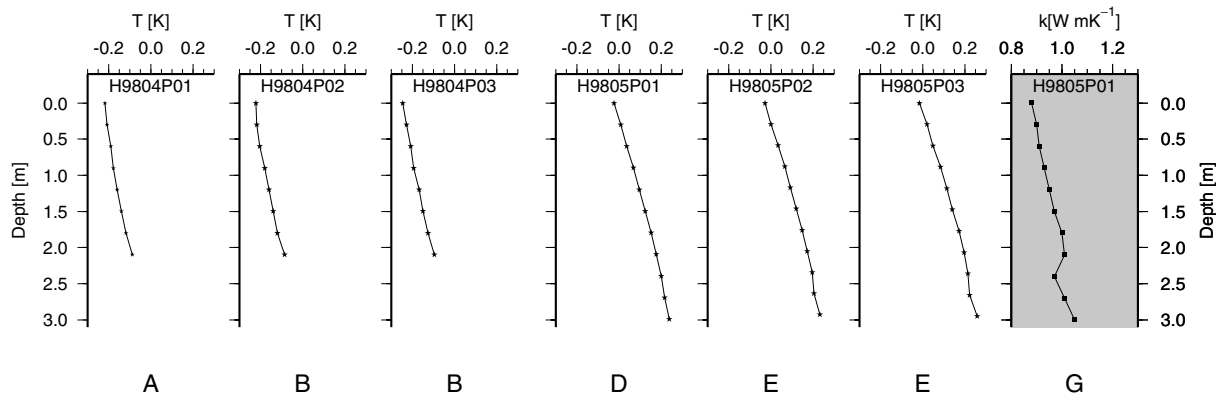


**Figure 4.** Temperature gradients measured at the upper (H9804) and middle (H9805) continental slope of the Laptev Sea. The measurements H9804P01–H9804P03 were taken in app. 520 m water depth (left) and show influence of transient effects introduced by water mass variations. The measurements H9805P01–H9805P03 were taken in app. 1500 m water depth. The plot G displays the results of *in situ* determinations of thermal conductivity.

shows the gradient of three penetrations (H9805P01–H9805P03), which were approximately 350 m apart. One measurement of thermal conductivity was performed at penetration H9805P01 indicating values of 0.9–1.1 W mK<sup>-1</sup> (see Fig. 4g).

### HEAT-FLOW CORRECTION

The heat-flow stations are located in an area of high sediment accumulation. Thus a correction for the reduced geothermal gradient owing to rapid sedimentation has to be applied.

The average sedimentation rate can be deduced from the thickness and age of the sedimentary cover. As the heat-flow stations are 20 km away from MCS line MAGE-90704, we have used a fragment of this line to estimate the total sedimentary thickness, which is approximately 2.3 km (2 s TWT) in the part of the profile where the heat-flow stations are projected to (Fig. 3c). To constrain possible time limits of the sedimentation we need to apply different assumptions drawn from models of opening of the Eurasia Basin according to Vogt *et al.* (1979), Karasik *et al.* (1983), Jackson & Johnson (1986), Savostin *et al.* (1984) and Drachev *et al.* (1988).

Since the heat-flow stations are located in the middle and upper continental slope, we assume that this area is underlain by a continental crust, though highly thinned during opening of the Eurasia Basin. The proximity of the heat-flow stations to the Khatanga–Lomonosov Fracture may suggest a significant contribution of shear to the crustal deformation in the area of the continental slope, as a result of the eastward Lomonosov Ridge during the course of the Cenozoic spreading in the Eurasia Basin (Fig. 5). Thus the subsidence at the heat-flow stations might have started as soon as the Lomonosov Ridge had passed the area of the heat-flow stations, which then came to face the oceanic basin.

As is known from published plate kinematic models, there are two major stages to the Eurasia Basin opening: relatively fast spreading between chrons 24 and 13 (53–33 Ma) followed by very slow spreading beyond the chron 13. The heat-flow stations are projected into that part of the Amundsen Basin, the crust of which is older than 33 Myr (Figs 2 and 3c). As the distances between the BSA and the anomaly A13, and BSA and the western flank of the Lomonosov Ridge measured along the seismic line MAGE-90704 parallel to the Khatanga–Lomonosov Fracture are 75 and 325 km, respectively, the calculated linear spreading rate for the Amundsen Basin for the period 53–33 Ma is 12.5 mm yr<sup>-1</sup>.<sup>2</sup> Since there is a distance of 123 km between the BSA and the heat-flow stations (Fig. 3c), the time when the western flank of the Lomonosov Ridge has passed heat-flow stations is calculated to be 43.2 Myr (Middle Eocene).

The Middle Eocene beginning of the sedimentation in the area of heat-flow stations is in contradiction with the seismic reflection data, which show the basement there to be overlain with the two uppermost seismic units (Fig. 3c). The age of these units can be inferred from the regional stratigraphy of the Laptev shelf region summarized by Grinenko (1989) since there are no drill holes over the entire Laptev Sea. These onshore data reveal a prominent hiatus at the Oligocene base in many key sections on the New Siberian Islands and around the Laptev Sea, while the overlying sediments demonstrate clear evidence of an Oligocene to Early Miocene regression (Drachev *et al.* 1998). In some areas this hiatus extends upsection to the Upper Miocene forming a prominent seismic unconformity offshore, indexed by Franke *et al.* (2001) as LS-3. Thus

<sup>2</sup>As the spreading in the Eurasia Basin is clearly asymmetric and faster in the Amundsen Basin, which is wider than the Nansen Basin, we have to use full opening rates for the Amundsen Basin instead of those for the entire Eurasia Basin.

we infer an Oligocene to Middle Miocene age for the SU-4, which was deposited at the sea level low stand, while the overlying SU-5 may correspond to a high sea level depositional environment during the Late-Miocene–Quaternary. Thus, the seismic data constrain indirectly the beginning of the sedimentation at heat-flow stations to the Early Oligocene (approximately 33–30 Ma). Both, seismic reflection and plate kinematic data give evidence that, though the Lomonosov Ridge might have passed the area of the heat-flow stations at approximately 43 Ma, this area had not been subsiding until 33 Ma, remaining a site of shearing deformation and probably denudation along the Khatanga–Lomonosov Fracture.

Accepting 33 Ma as the beginning of sedimentation in the area of the heat-flow stations we can calculate 0.07 mm yr<sup>-1</sup> to represent an average sedimentation rate. This estimated value agrees well with the sedimentation rates from 0.04 to 0.5 mm yr<sup>-1</sup> for the last 12 kyr, derived from several sediment cores recovered from the continental slope of the Laptev Sea (Stein *et al.* 1999).

The reduction of the thermal gradient by sedimentation was estimated according to Jessop (1990). Fig. 6 depicts the graphs for continuous sedimentation rates for 0.01, 0.07 and 0.1 mm yr<sup>-1</sup> over time. 31.6–33.6 Myr of continuous sedimentation at a 0.07 mm yr<sup>-1</sup> rate leads to a reduction of the thermal gradient to 0.83 of its original value. This yields a reduction of approximately 17 per cent. Applying this correction yields heat-flow values of 85–117 mW m<sup>-2</sup>. In comparison, assuming a crustal cooling model after Parsons & Sclater (1977) for the 33 Myr old crust would yield a maximum value of 83 mW m<sup>-2</sup>.

Corrections owing to rapid sedimentation caused by hang slides or turbidity currents may apply. These corrections are even more difficult to quantify because of the lack of high-resolution sediment profiles or cores. Nevertheless, all the corrections would have the same effect: to increase the actual values. Thus values given here, uncorrected and with the sediment correction applied, are minimum estimates.

A terrain correction was calculated for the continental margin according to the approach of Lachenbruch (1968). The overall slope of the margin according to IBCAO data (International bathymetric chart of the Arctic Ocean Jakobsson *et al.* 2000) does not exceed an angle of 2°, resulting in a correction of less than 2 per cent, which can be neglected within our error bounds.

Occurrences of water discharge are simply not known and cannot be deduced from the data.

### DISCUSSION

The fact that the structural elements of the easternmost Eurasia Basin are overlain by sediments and are not manifested in the sea bottom morphology has been used by Sekretov (2002) to suggest a degeneration of the Gakkel Ridge towards the LSCM and cessation of the spreading itself for the last 33 Myr. However, the available data sets, presented partly in this paper, not only reveal the buried spreading axis but also show evidence of continued and ongoing extension under a thick sedimentary cover.

According to the MCS profiles and the gravity field, the BSA can be continuously traced under the sedimentary pile of the eastern Eurasia Basin up to 2500 m isobath. Furthermore, in the area of the continental slope the BSA appears as two asymmetric grabens, around which the hydrothermal fauna and the high heat-flow values are found. Thus we attribute these grabens to the buried spreading axis of the Gakkel Ridge and consider them as a finite segment of the global Atlantic–Arctic spreading system abutting the Khatanga–Lomonosov Fracture.

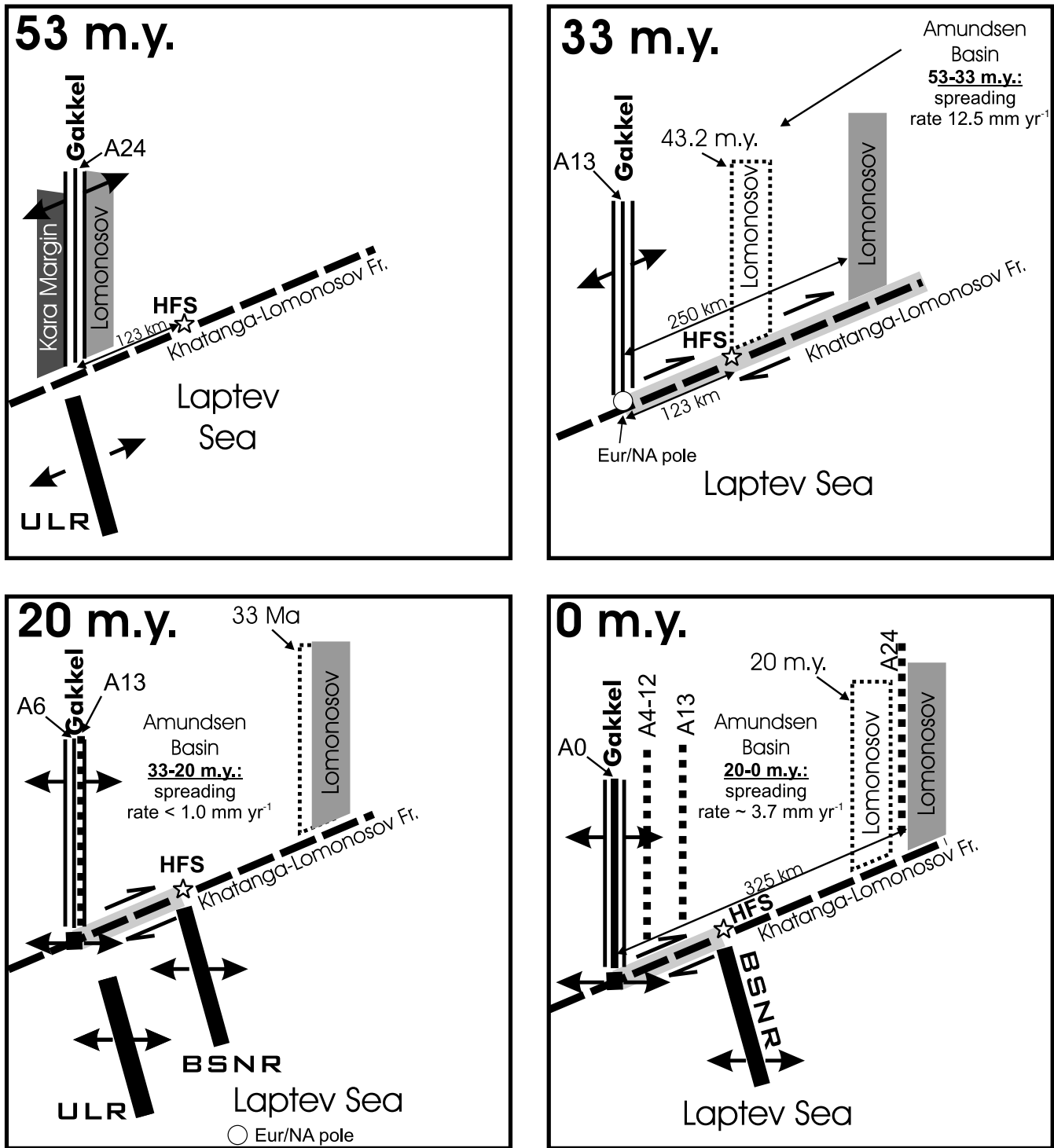
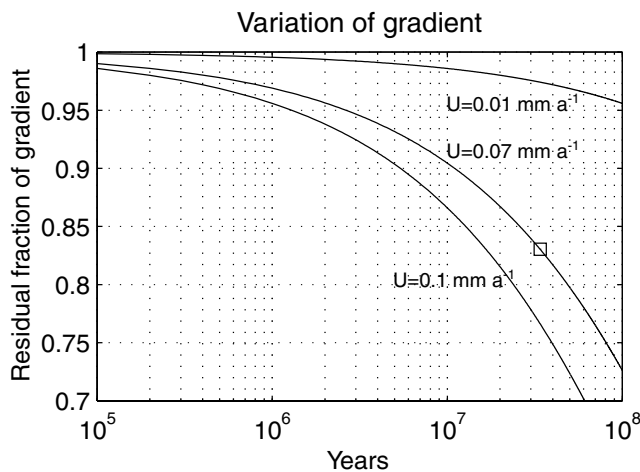


Figure 5. Spreading model for opening of the eastern Eurasia Basin. HFS—heat flow stations, Eur/NA—Eurasian/North American plates, UR—Ust’ Lena Rift, BSNR—Bel’kov–Svyatoi Nos Rift. The active shear deformations along the Khatanga–Lomonosov Fracture are marked by a grey strip.

Though a thinned and detached continental crust might still be present beneath the continental slope, we assume that this region is mostly affected by a spreading-driven extension. This suggestion is based on the obvious necessity to apply a northeastern movement of the Lomonosov Ridge with regard to the LSCM during opening of the Eurasia Basin (Drachev *et al.* 1998; Drachev 2000). Probably the whole continental slope represents a zone of transension dislocations generated by the spreading and a shear-type movement of the

southern Lomonosov Ridge along the LSCM while the whole ridge was moving away from its pre-spreading position at the Barents–Kara continental margin (Fig. 5). Thus the Khatanga–Lomonosov Fracture, which separates the spreading Eurasia Basin from a continental shelf rift system, may have been accommodating this lateral movement.

The heat-flow-probed area is located at the middle to upper continental slope just northward of the Khatanga–Lomonosov



**Figure 6.** Reduction of thermal gradient according to sedimentation rate (after Jessop 1990). Horizontal axis depicts the time in years since beginning of sedimentation and vertical axis the remaining portion of heat flow gradient. Three graphs for sedimentation rates of  $0.01 \text{ mm yr}^{-1}$  (lower limit),  $0.07$  (chosen mean) and  $0.1 \text{ mm yr}^{-1}$  (upper limit) are displayed. The rectangle indicates the result (83 per cent) for chosen values (33 Ma,  $0.07 \text{ mm yr}^{-1}$ ).

Fracture. So it might suffer strong shearing during the first stage of the Eurasia Basin opening (53–33 Ma, Fig. 5). Despite that the western Lomonosov flank has passed this site by 43 Ma and since that time it has been located in the vicinity of the oceanic basin, the active tectonic movements may have been provoking the local uplift and denudation. At 33 Ma a change in the global plate movement took place, so the pole of North American/Eurasian plate rotation is found for this time at the eastern termination of the Eurasia Basin (Karasik *et al.* 1983; Savostin *et al.* 1984; Savostin & Drachev 1988) where it has remained for the next 13 Myr (Fig. 5). This event led to compression in many places of the Laptev Sea Region (Drachev *et al.* 1998), while within the eastern Eurasia Basin the plate divergence continued, but at a very low rate (approximately  $1 \text{ mm yr}^{-1}$ ). In this regime of tectonic stagnation the area of heat-flow probing was probably subjected to a subsidence as shown by the seismic reflection data. At approximately 20 Ma the plate divergence at the Eurasia Basin/Laptev Shelf transition was gradually increased again as the pole of plate rotation had been moving southward. It triggered normal faulting at the continental slope continuation of the buried spreading axis and significant subsidence within the area of the heat-flow measurements and accumulation of the seismic unit 5. Within the continent, this phase of extension in the Late-Miocene to Pliocene caused the appearance of the large Cherskii Arch, complicated by the axial Moma Rift (Fig. 7).

Heat-flow values were previously measured at a few sites around the Laptev Sea. Most of them are included in a global database (Pollack *et al.* 1993, see also [www.geo.lsa.umich.edu/IHFC/heatflow.html](http://www.geo.lsa.umich.edu/IHFC/heatflow.html)). However, no heat-flow values have been recovered for the entire Laptev Shelf so far. This is partly because of the presence of a permafrost layer beneath the Holocene marine sediments, proved recently by shallow offshore drilling (Kassens *et al.* 2000). This prevents a determination of the true basal thermal gradient from the few surface measurements on the Laptev Sea Shelf. The only three known values exist just onshore where wells have been drilled deep enough to penetrate the permafrost. These are:  $53 \text{ mW m}^{-2}$  near the Lena Delta (Tiksi Well),  $50 \text{ mW m}^{-2}$  in the northern part of Bol'shoi Lyakhov Island and  $46 \text{ mW m}^{-2}$  close to Omoloi Graben, which is an onshore continuation of the Ust' Lena Rift (Fig. 7).

More heat-flow observations are known in the areas south of the Laptev Sea. Most of them are shown in Fig. 7. From deep drill holes, Duchkov (1991) deduces a background heat flow of  $38 \text{ mW m}^{-2}$  for the Siberian Craton comprising an area from the Kara Sea to the Lena River. The northern part of the craton reveals a mean heat-flow values of  $20 \text{ mW m}^{-2}$ . The low heat flow is attributed to the fact that this platform area has been tectonically stable for more than the past 200 Myr.

The area east of the Siberian Craton has a significantly larger heat flow. This younger tectonic province was built up by the Late Mesozoic fold belts, which were affected by crustal extension in the Late Cenozoic along the Cherskii Range (Grachev 1982; Cook *et al.* 1986; Parfenov *et al.* 1988; Fujita *et al.* 1990a; Paech *et al.* 1998). The high heat-flow values are found near the Moma Rift, which is a zone of young elongated depressions, basalt volcanism and hot springs (Argunov & Gavrikov 1960; Naymark 1976). Grachev (1999), on the basis of the geochemistry of the recent basalts of Northeastern Asia, postulates that this area is influenced by a mantle plume, which is under an initial stage of development.

The heat flow measured at the continental slope of the LSCM is considerably higher than is known from an onshore 'hot' region. The revealed actual basal heat-flow values of  $85\text{--}117 \text{ mW m}^{-2}$  exceed the regional background value  $38 \text{ mW m}^{-2}$  by a factor of 2.5. The hydrothermal site at the southern termination of the Gakkel Ridge identified by assemblages of bivalve shells indicates a high heat flux in conjunction with a fluid drainage site. Both a high heat flow and hydrothermal benthos are typical for a spreading axis environment and can be considered as evidence of ongoing extension at the upslope prolongation of the BSA.

## CONCLUSION

The northern Laptev Sea is one of the few places globally where a currently active spreading ridge approaches a continental margin. Because of its tectonic setting this region represents a unique natural laboratory for addressing the processes of the breakup of continents and their impact on the natural environment. Significant progress in studying the spreading ridge/continental margin intersection in the Laptev Sea has been achieved over the past ten years. New geophysical observations, primarily the Russian and German multichannel seismic reflection data, ERS-1 and ERS-2 satellite altimeter-derived gravity field and heat-flow measurements, have shed more light on this unique tectonic junction.

Based on seismic reflection and gravity data, the spreading axis of the Gakkel Ridge is traced under a thick Cenozoic sedimentary cover of the eastern Eurasia Basin up to the continental rise, representing the unique occurrence of a sediment-covered ultraslow spreading axis. Its further continuation into the area of the continental slope can be attributed to two asymmetric grabens, which terminate against the prominent Khatanga–Lomonosov Fracture. Hydrothermal faunal remnants and the high heat flow ( $85\text{--}117 \text{ mW m}^{-2}$ ) documented around these grabens in the up-slope area are typical characteristics for an oceanic divergent axis. Thus we consider these grabens as an extreme end of the global Atlantic–Arctic spreading system.

In a modern tectonic setting the Laptev Sea is an area of interaction between the North American and Eurasian lithospheric plates. The geometry of the southward continuation of the divergent plate boundary as it passes from the Eurasia Basin on to the Laptev Shelf can only be inferred from seismologic data and multichannel seismic reflection surveys. Probably, as has already been mentioned by Drachev (2000) and Franke *et al.* (2000), the buried spreading axis of the Gakkel Ridge does not penetrate directly through the



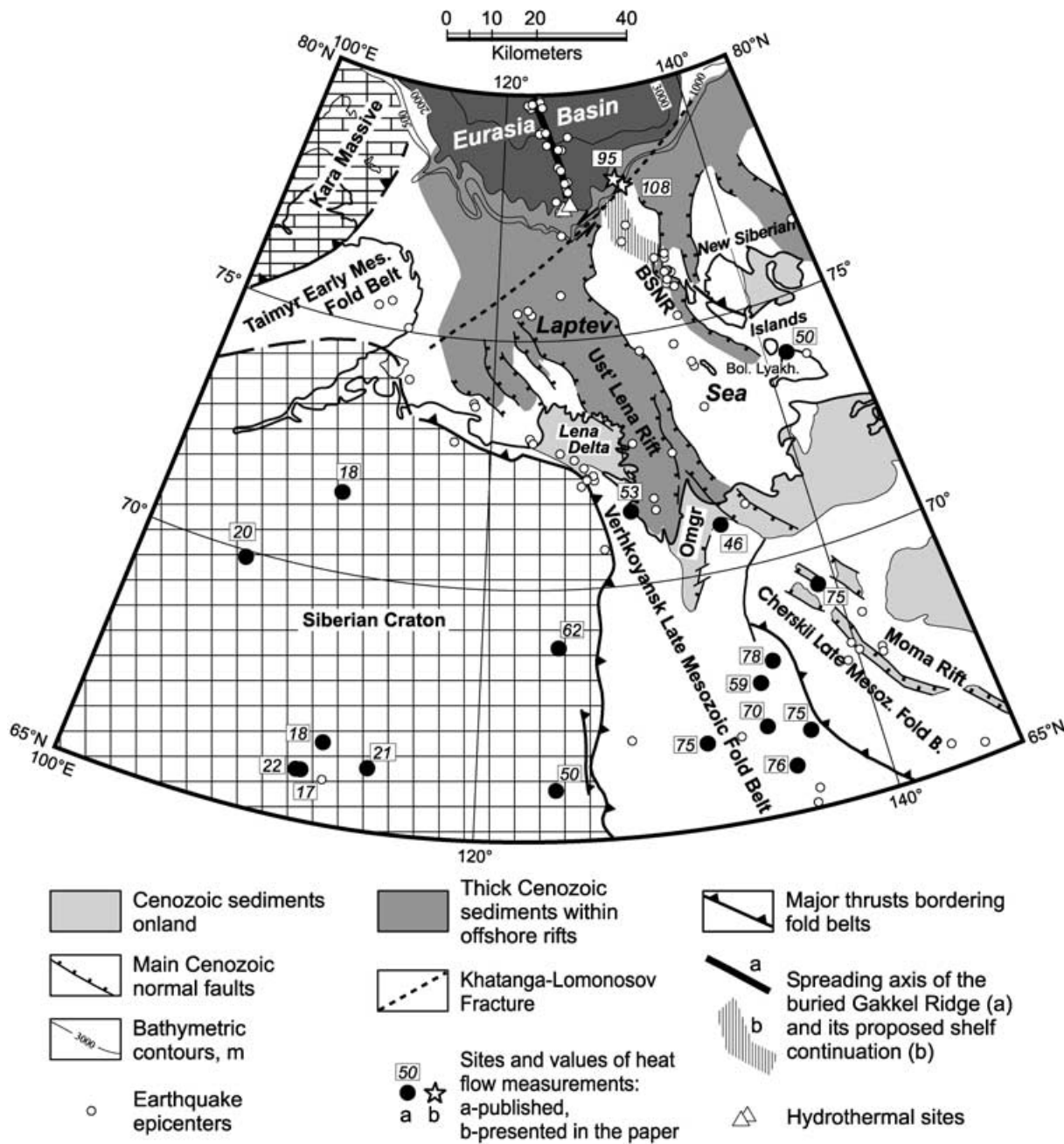


**Figure 7.** Main structural elements, seismicity and heat flow of the Laptev Sea Region and surrounding areas. Heat flow values (Pollack *et al.* 1993) increase toward the buried Gakkel Ridge-Laptev Rift System-Moma Rift, which are the locus of the North American-Eurasian plates interaction. Polar stereographic projection. BSNR—Bel’kov–Svyatoi Nos Rift, Omgr—Omoloi Graben.

Khatanga–Lomonosov Fracture and spreading is not taking place within the shelf. A linear narrow zone of seismicity follows the Gakkel Ridge rift valley and then turns to the Western Graben at the continental slope. Further shelf continuation of the divergent plate boundary can be inferred westward of the New Siberian Islands where a high seismicity zone corresponds to the northern part of the Bel’kov–Svyatoi Nos Rift. Distribution of the earthquake epicentres, increased heat flow and currently active normal faults allow us to assume a 140–150 km eastward offset of the present-day divergent plate boundary in the area of the Eurasia Basin–Laptev Sea transition along the Khatanga–Lomonosov Fracture. Further to the south the plate boundary is found in the Cherskii Mountain Belt, as shown by Savostin & Karasik (1981), Grachev (1982), Cook *et al.*

(1986), Parfenov *et al.* (1988), Fujita *et al.* (1990a) and Franke *et al.* (2000).

**ACKNOWLEDGMENTS**

This work is one of the results of long-term Russian–German cooperation within the framework of the research programme ‘Laptev Sea System 2000’. We are grateful to J. Thiede and W. Jokat (Alfred Wegener Institute, FRG) and L. Johnson (Alaskan University, Fairbanks), whose well-meant critical comments helped to improve the whole paper. We are also in debt to D. Franke and A. Duchkov whose reviews helped to clarify the text. This work was supported by the German–Russian Otto Schmidt Laboratory

(grant OSL-011), Russian Basic Research Foundation (grant 01-05-64979) and the German Ministry of Education and Research (grant 03G0534).

## REFERENCES

- Argunov, M.S. & Gavrikov, S.I., 1960. Balagan-Tas, an early Quaternary volcano. *Izv. Acad. Sci. USSR*, **8**, 72–74.
- Argus, D.F. & Heflin, M.B., 1995. Plate motion and crustal deformation estimated with geodetic data from the global positioning system. *Geophys. Res. Lett.*, **22**, 1973–1976.
- Avetisov, G.P., 1999. Geodynamics of the zone of continental continuation of Mid-Arctic earthquakes belt (Laptev Sea). *Phys. Earth planet. Inter.*, **114**, 59–70.
- Bauch, H.A., Kassens, H., Erlenkeuser, H., Grootes, P.M. & Thiede, J., 1999. Depositional environment of the Laptev Sea (Arctic Siberia) during the Holocene. *Boreas*, **28**, 194–204.
- Cande, S.C. & Kent, D.V., 1995. Revised calibration of the geomagnetic polarity timescale for the Late Cretaceous and Cenozoic. *J. geophys. Res.*, **100**, 6093–6095.
- Cook, D.B., Fujita, K. & McMullen, C.A., 1986. Present-day plate interactions in Northeast Asia: North American, Eurasian, and Okhotsk plates. *J. Geodyn.*, **6**, 33–51.
- Demenitskaya, R.M. & Karasik, A.M., 1969. The active rift system of the Arctic Ocean. *Tectonophysics*, **8**, 345–351.
- DeMets, C., Gordon, R.G., Argus D.F. & Stein S., 1990. Current plate motions. *Geophys. J. Int.*, **101**, 425–478.
- Drachev, S.S., 1998 (printed 2000). Laptev Sea Rifted Continental Margins: modern knowledge and unsolved questions. *Polarforschung*, **68**, 41–50.
- Drachev, S.S., 2000. Tectonics of the Laptev Sea Rift System. *Geotectonics*, **6**, 43–58 (in Russian).
- Drachev, S.S., Savostin, L.A., Groshev, V.G. & Bruni, I.E., 1998. Structure and geology of the continental shelf of the Laptev Sea, Eastern Russian Arctic. *Tectonophysics*, **298**, 357–393.
- Drachev, S.S., Johnson, G.L., Laxon, S., McAdoo, D. & Kassens, H., 1999. Main structural elements of the Eastern Russian Arctic Continental Margin derived from satellite gravity and multichannel seismic reflection data, in *Land–Ocean Systems in the Siberian Arctic: Dynamics and History*, pp. 667–682, eds Kassens, H. et al., Springer, Berlin.
- Duchkov, A.D., 1991. Review of Siberian heat flow data, in *Terrestrial Heat Flow and the Lithosphere Structure*, pp. 426–443, eds Cermak, V. & Rybach, L., Springer, Berlin.
- Franke, D., Hinz, K., Block, M., Drachev, S.S., Neben, S., Kos'ko, M.K., Reichert, C. & Roeser, H.A., 1998 (erschienen 2000). Tectonics of the Laptev Sea Region in Northeastern Siberia. *Polarforschung*, **68**, 51–58.
- Franke, D., Krüger, F. & Klinge, K., 2000. Tectonics of the Laptev Sea–Moma 'Rift' region: investigation with seismological broadband data. *J. Seismol.*, **4**, 99–116.
- Franke, D., Hinz, K. & Oncken, O., 2001. The Laptev Sea Rift. *Mar. Geol.*, **18**, 1083–1127.
- Fujita, K., Cambray, F.W. & Velbel, M.A., 1990a. Tectonics of the Laptev Sea and the Moma rift systems, northeastern USSR, in *Arctic Geoscience. Mar. Geol.*, Vol. 93, pp. 95–118, eds Weber, A.F., Forsyth, D.A., Embry, A.F. & Blanco, S.M.
- Fujita, K., Cook, D.B., Hasegawa, H., Forsyth, D. & Wetmiller, R., 1990b. Seismicity and focal mechanisms of the Arctic region and the North American plate boundary in Asia, in *The Geology of North America*, Vol. L., The Arctic Ocean region, pp. 79–100, eds Grantz, A., Johnson, L. & Sweeney, J.F., Geol. Soc. of Amer., Boulder, CO.
- Fütterer, D.K., 1994. Die Expedition ARCTIC '93. Der Fahrtabschnitt ARK-IX/4 mit FS Polarstern 1993. *Ber. Polarforsch.*, **149**, 124.
- Glebovsky, V.Yu., Kovaks, L.C., Mashchenkov, S.P. & Brozena, J.M., 1998 (erschienen 2000). Joint compilation of Russian and US Navy aeromagnetic data in the central Arctic seas. *Polarforschung*, **68**, 35–40.
- Grachev, A.F., 1982. Geodynamics of the transitional zone from the Moma Rift to the Gakkel Ridge, in *Studies in Continental Margin Geology*, Vol. 34, pp. 103–113, eds Watkins, J.S. & Drake, C.L., Am. Assoc. Pet. Geol. Mem.
- Grachev, A.F., 1999. Quaternary volcanism and geodynamics issues of North-Eastern Asia. *Fizika Zemli*, **9**, 19–37 (in Russian).
- Grachev, A.F., Demenitskaya, R.M. & Karasik, A.M., 1970. Mid Arctic Ridge and their continental continuation. *Geomorphologiya*, **1**, 42–45 (in Russian).
- Grinenko, O.V., (ed.), 1989. Paleogene and Neogene of North-East of the USSR, Scientific Center of Siberian Department of Academy of Sciences of USSR, Yakutsk, p. 184 (in Russian).
- Jessop, A.M., 1990. *Thermal Geophysics*, Elsevier, Amsterdam, p. 306.
- Hartmann, A. & Villinger, H., 2002. Inversion of marine heat-flow measurements by expansion of the temperature decay integral. *Geophys. J. Int.*, **148**, 628–636.
- Hyndman, R.D., Davis, E.E. & Wright, J.A., 1979. The measurement of marine geothermal heat flow by a multipenetration probe with digital acoustic telemetry and *in situ* thermal conductivity. *Mar. geophys. Res.*, **4**, 181–205.
- Ivanova, N.M., Sekretov, S.B. & Shkarubo, S.N., 1990. Geological structure of the Laptev Sea shelf according to seismic studies. *Oceanology*, **29**, 600–604.
- Jakobsson, M., Macnab, R. & Members of the Editorial Board, 2000. International Bathymetric Chart of the Arctic Ocean, beta version. <http://www.ngdc.noaa.gov/mgg/bathymetry/arctic/arctic.html>, p. 14.
- Karasik, A.M., 1974. The Eurasia Basin of the Arctic Ocean from the point of view of plate tectonics, in *Problems in Geology of Polar Areas of the Earth*, Leningrad, Nauchno-Issledovatel'skii Institut Geologii Arktiki, pp. 23–31 (in Russian).
- Karasik, A.M. & Sochevanova, N.A., 1990. *Linear Magnetic Anomalies of the World Ocean*, International geological and geophysical atlas of the Atlantic Ocean. Moscow, sheet 48.
- Karasik, A.M., Savostin, L.A. & Zonenshain, L.P., 1983. Parameters of the lithospheric plate movements within Eurasia Basin of North Polar Ocean. *Dokl. Acad. Nauk SSSR, Earth Sci. Sect.*, **273**, 1191–1196 (in Russian).
- Kassens, H. et al., 2000. First Impressions of TRANSDRIFT VIII expedition to the Laptev Sea: the shelf drilling campaign of 'Laptev Sea System 2000'. *6th Workshop on Russian-German Cooperation: Laptev Sea System*. St Petersburg, Russia, October 12–14, 2000. Program and Abstracts, *Terra Nostra*, **2000/8**, 39–40.
- Kristoffersen, Y., 1990. Eurasia Basin, in *The Geology of North America*, Vol. L., The Arctic Ocean region, pp. 365–378, eds Grantz, A., Johnson, L. & Sweeney, J.F., Geol. Soc. of Amer., Boulder, CO.
- Lachenbruch, A.H., 1968. Rapid estimation of the topographic disturbance to superficial thermal gradients. *Rev. Geophys. Space Phys.*, **6**, 365–400.
- Laxon, S. & McAdoo, D., 1994. Arctic Ocean gravity field derived from ERS-1 satellite altimetry. *Science*, **265**, 621–624.
- Laxon, S.W. & McAdoo, D.C., 1998. Satellites provide new insights into Polar geophysics. *EOS, Trans. Am. geophys. Un.*, **79**, 72–73.
- Naymark, A.A., 1976. Neotektonics of the Moma region, northeastern USSR. *Trans. USSR Acad. Sci., Earth Sci. Sect.*, **229**, 39–42.
- Paech, H., Prokopiev, A.V., Gosen, W.V., Grinenko, O.V., Smetannikova, L.I. & Belolyubskij, I.N., 1998 (erschienen 2000). New Results of the Moma Rift System and Coeval Structures in Yakutia, Russian Federation. *Polarforschung*, **68**, 59–63.
- Parfenov, L.M., Koz'min, B.M., Grinenko, O.V., Imaev, V.S. & Imaeva, L.P., 1988. Geodynamics of the Chersky seismic belt. *J. Geodyn.*, **9**, 15–37.
- Parsons, B. & Sclater, J.G., 1977. An analysis of the variation of ocean floor bathymetry and heat flow with age. *J. geophys. Res.*, **82**, 803–827.
- Patyk-Kara, N.G. & Grishin, M.A., 1972. Position of the Polousnyy Range in the structure of the northeast USSR and its most recent tectonics. *Geotectonics*, **6**, 242–245.
- Petryashov, V.V., Sirenko, B.I., Rachor, E. & Hinz, K., 1994. Distribution of macrobenthos in the Laptev Sea from the materials of the expeditions

- aboard the hydrographic ship 'Ivan Kireev' and the icebreaker 'Polarstern' in 1993, in *Nauchnye rezul'taty ekspeditsii LAPEKS-93*, St Petersburg, Gidrometeoizdat, pp. 277–288 (in Russian).
- Pollack, H.N., Hurter, S.J., Johnson, J.R., 1993. Heat flow from the Earth's interior: analysis of the global data set, *Rev. Geophys.*, **31**, 267–280.
- Roeser, H.A., Block, M., Hinz, K. & Reichert, C., 1995. Marine geophysical investigations in the Laptev Sea and the western part of the East Siberian Sea, *Ber. Polarforschung*, **176**, 367–377.
- Rudels, B., Jones, E.P., Anderson, L.G. & Kattner, G., 1994. On the intermediate depth waters of the Arctic Ocean, in *Polar Oceans and Their Role in Shaping the Global Environment*, pp. 33–46, eds Johannessen O.M. *et al.*, AGU, Washington, DC.
- Savostin, L.A. & Drachev, S.S., 1988. The Cenozoic compression in New Siberian Island Region and its Relationship with Eurasia Basin opening, *Oceanologiya*, **28**, 775–782 (in Russian).
- Savostin, L.A. & Karasik, A.M., 1981. Recent plate tectonics of the Arctic basin and of northeastern Asia, *Tectonophysics*, **74**, 111–145.
- Savostin, L.A., Karasik, A.M. & Zonenshain, L.P., 1984. The history of the opening of the Eurasian basin in the Arctic, *Trans. USSR Acad. Sci. Earth Sci. Sect.*, **275**, 79–83.
- Sekretov, S.B., 2002. Structure and tectonic evolution of the Southern Eurasia Basin, Arctic Ocean, *Tectonophysics*.
- Sirenko, B.I., Petryashov, V.V., Rachor, E. & Hinz, K., 1995. Bottom bio-coenoses of the Laptev Sea and adjacent areas, *Ber. Polarforschung*, **176**, 211–221.
- Stein, R., Fahl, K., Niessen, F. & Stiebold, M., 1999. Late Quaternary organic carbon and biomarker records from the Laptev Sea continental margin (Arctic Ocean): implications for organic carbon flux and composition, in *Land–Ocean Systems in the Siberian Arctic: Dynamics and History*, pp. 635–655, eds Kassens, H. *et al.*, Springer, Berlin.
- Verhoef, J., Walter, R.R., Macnab, R., Arkani-Hamed, J. & Members of the Project Team, 1996. Magnetic anomalies of the Arctic and North Atlantic oceans and adjacent land areas, Geological Survey of Canada. Open File 3125a.
- Vinogradov, V.A., 1984. The Laptev Sea, in *Geologic Structure of the USSR and its Relationship to the Distribution of Mineral Resources*, Vol. 9, Seas of the Soviet Arctic, pp. 51–60, eds Gramberg, I.S. & Pogrebetskii, Y.E., Nedra, Leningrad (in Russian).
- Vogt, P.R., Taylor, P.T., Kovacs, L.C. & Johnson, G.L., 1979. Detailed aeromagnetic investigation of the Arctic Basin, *J. geophys. Res.*, **84**, 1071–1089.
- Zonenshain, L.P., Natapov, L.M., Savostin, L.A. & Stavskii, A.P., 1978. Recent plate tectonics of the northeastern Asia in connection with the opening of North Atlantic and the Arctic Ocean basins, *Oceanology*, **18**, 550–555.